NGU Report 2008.049

Field studies of unstable slopes in Sunndalen Valley

Geological Survey of Norway
NO-7441 Trondheim, Norway
Tel.: 47 73 90 40 00
Telefax 47 73 92 16 20

REPORT

Report no.: 2008.049 | ISSN 0800-3416 | Grading: Open

Title:
Field studies of unstable slopes in Sunndalen Valley

Authors:
Saintot, A., Böhme, M., Redfield, T., Dahle, H.

Client:
Møre og Romsdal Fylke

County:
Møre og Romsdal

Commune:
Sunndalsøra

Map-sheet name (M=1:250.000)
Ålesund, Røros

Map-sheet no. and -name (M=1:50.000)

Deposit name and grid-reference:

Number of pages: 26 Price (NOK): 190
Map enclosures:

Fieldwork carried out: 2007

Date of report: August 2008

Project no.: 309900

Person responsible: Lars A. Blikra

Summary:

Following a helicopter survey of the slopes along the Sunndalen valley and the surroundings in spring 2007, four sites have been selected for further field studies. Two sites, (Gikling and Ottem), were mapped during summer 2007. GPS points for yearly monitoring were emplaced at Gikling. The volume of the unstable slope may be as much as 100 Mm^3. At Ottem, a slope instability of about 2 Mm^3 was mapped in detail. Scree deposits comprising large blocks along the slope are also unstable. GPS monitoring points were selected at Ottem and will be set out in 2008. Also at Ottem, another larger zone has been observed on aerial photographs. Gravitational fractures appear to have developed along a fold hinge at the edge of the high plateau. This zone should be checked in 2008. The two other sites (Hårstad and Ivasnasen) have been initially examined from their toe zone; detailed field mapping will be undertaken in 2008. The estimated unstable volumes at these two sites are about 5 Mm^3. A fifth site called Vollan has been observed on aerial photographs during winter 2007/2008. The deformed area may cover a large area of 1 to 2 km^2 and field investigations of this area are necessary in 2008.

Keywords: Slope instability	Mapping	Møre og Romsdal
Sunndalen	rock avalanches	rockslides

CONTENTS

FIGURES

Figure 8. Orthophoto (www.norgeibilder.no) of the unstable slope of Ottem and maps of structures. On the eastern part of the studied area, a fold hinge localizes a possible large unstable zone (sector 1). Part of the scarp has already failed and the scree deposits on the slope are unstable loose material that comprises large blocks (sector 2). The western edge of the plateau at about 1000 m a.s.l. is unstable (sector 3) and cracks developed from east to west at the back.

Figure 9. Field photos. A, view of the face of the unstable zone (sectors 2 and 3 of Figure 8). B, view parallel to the propagating back-fracture at the back of the unstable block (sector 3 of Figure 8). Note the large opening of the crack seen along the cliff. C, the collapsing unstable block (sector 3) with the back-crack underlined in yellow. The back-crack is well developed and opened on its eastern side whereas on the western side it is a linear depression highlighted by a series of small ponds.

Figure 10. Stereoplots of structural data collected at Ottem on the unstable block of sector 3 (see Figure 8). Locations of field measurements as white dots; GPS points to be established in 2008 as green squares; legend for stereoplots as in Figure 4 (measurements are listed in Appendix 1). The red lines are the limits of the block. The dashed lines are the depressions seen in the field and are the supposed limits of the blocks.

Figure 11. General top view of the site of Hårstad (from www.norgei3d.no). In the northern zone, the failure of the slope consists of columns and slices toward an E-W trending tributary river. On the southern zone, large blocks slid eastward toward the main valley on shallow east–dipping foliation, detachment of block A being more advanced than for block B.

Figure 12. A, Some photos that give an overview of the site of Hårstad with the two types of instabilities (as for Figure 11, North is to the right). B, sliding blocks along reactivated shallow dipping foliation planes (in red dashed lines); open steep fractures (in blue dashed lines) testify to displacement. C, general view of the slices and columns that detached toward an E-W gully. D, NW-SE cracks (at the tip of the red arrows) along which the slices and columns detached. E, view of the large columns that detached toward the E-W gully with volumes of approximately 0,25 Mm^3.

Figure 13. Geological map of Vollan and Ivasnasen surroundings (scale 1 /250 000, Nilsen, O. and Wolff, 1989). Note that sector 1 is a promontory in the topography called Ivasnasen, with three free borders that may favor the destabilization of the whole volume.

Figure 14. A, 3D view with orthophotos of the slope instability at Gjøra and Ivasnasen surroundings (www.norgei3d.no) and locations of the different parts of the instability. B, northeastern part of the limit of the previous failed volume and slope instability that propagates towards the north-east (sector 2 of Figure 13). C, southwestern slope instability called Ivasnasen (sector 1, Figure 13) and open NE-SW fractures that have propagated from the failed back-crack. D, southern face of Ivasnasen, the southwestern slope instability (sector 1 of Figure 13). The rock face displays ductile folds but also brittle structures. A detailed mapping of the site will be performed in 2008.

Figure 15. Aerial photograph of the Vollan site with indications of minimum and maximum boundaries of the slope instability. (www.norgeibilder.no)

Figure 16. Topographic map of the Vollan site showing the break of the slope angle.

INTRODUCTION

Sunndalen is a ~35 km long, WNW-ESE orientated, steep-sloped, U-shaped glacial valley. Eleven historical slope failures have been identified along the Sunndalen valley and its surroundings (Figure 1). E. Anda and L.H. Blikra have already identified two new gravitational slope instabilities, Gikling and Ottem, (NGU database) using aerial photograph analyses and a helicopter survey. The past events and the observations of such present instabilities were the motivation for a new helicopter survey in spring 2007.

Ottem and Gikling were mapped in detail during August 2007; the results of the field investigations are presented in this report. All measurements of the structural field data are listed in Appendix 1. In addition to these new field surveys at Gikling and Ottem, two other sites were identified during the helicopter survey: Hårstad and Ivasnasen (Figure 1). They are documented in this report using aerial photograph and Digital Elevation Model data coupled with direct observations of the slopes from the bottom of the valley. Another large slope instability (herein named Vollan) was observed on aerial photographs during the winter of 2007 and is subsequently documented in this report. These three zones are targets for detailed investigations during the 2008 field season.

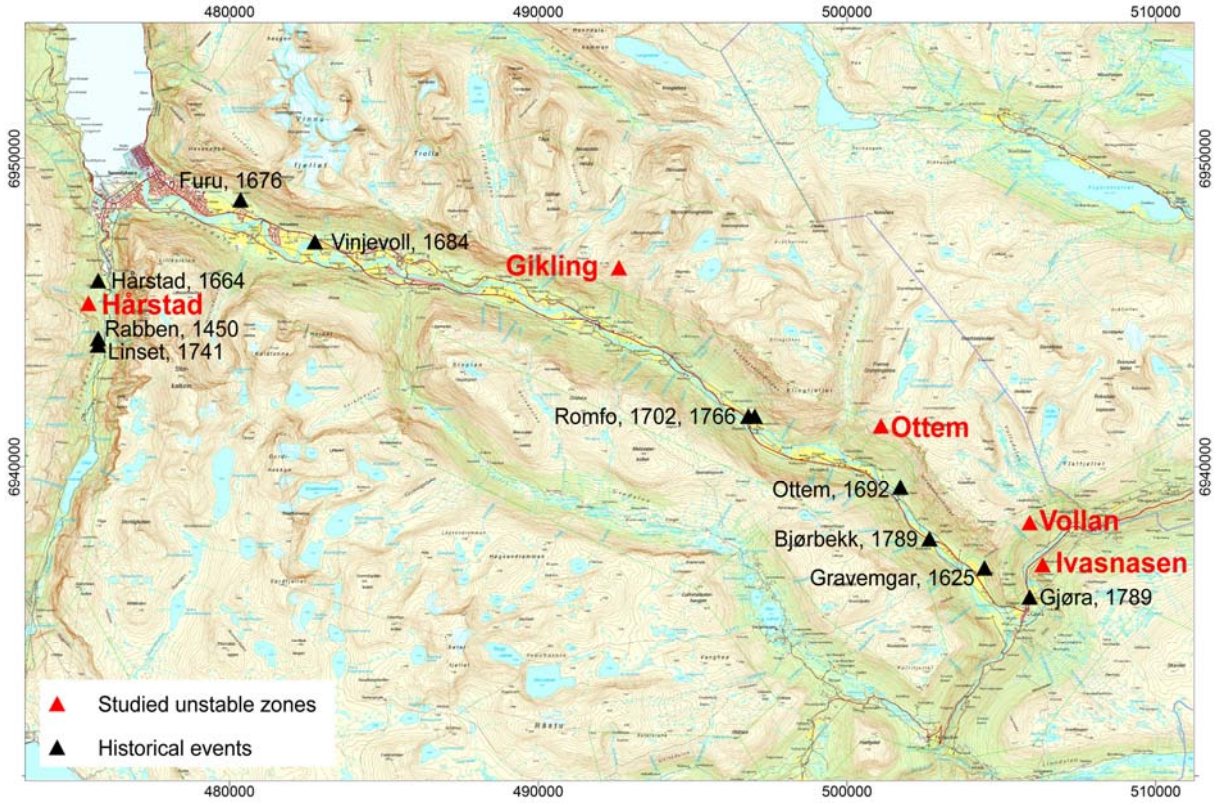

Figure 1. Topographic map of the study area showing both the historical slope failures (skrednett.no database) and the studied sites with respect to the transportation system and main population centers.

1. GEOLOGICAL SETTING

The Sunndalen region is underlain by three gneissic tectonic units (Figure 2). The Sunndalen valley itself was carved into two Precambrian gneiss units of the autochthonous basement, now separated by a vertical tectonic contact. The autochthonous unit in the eastern part of the valley contains micaschist lenses that locally crosscut the valley. To the north lies a nappe of

middle allochthonous units including Precambrian granitic to dioritic gneiss. The contact with the underlying autochthonous basement is a flat to very low angle thrust incorporating a thin layer of metasandstones and schists (Figure 2). The easternmost part of the studied area consists of a NE-SW trending narrow band of 4 different, very attenuated tectonic units belonging to the autochthon, as well as the middle, and upper –allochthons. The contacts between each tectonic units are large fault zones.

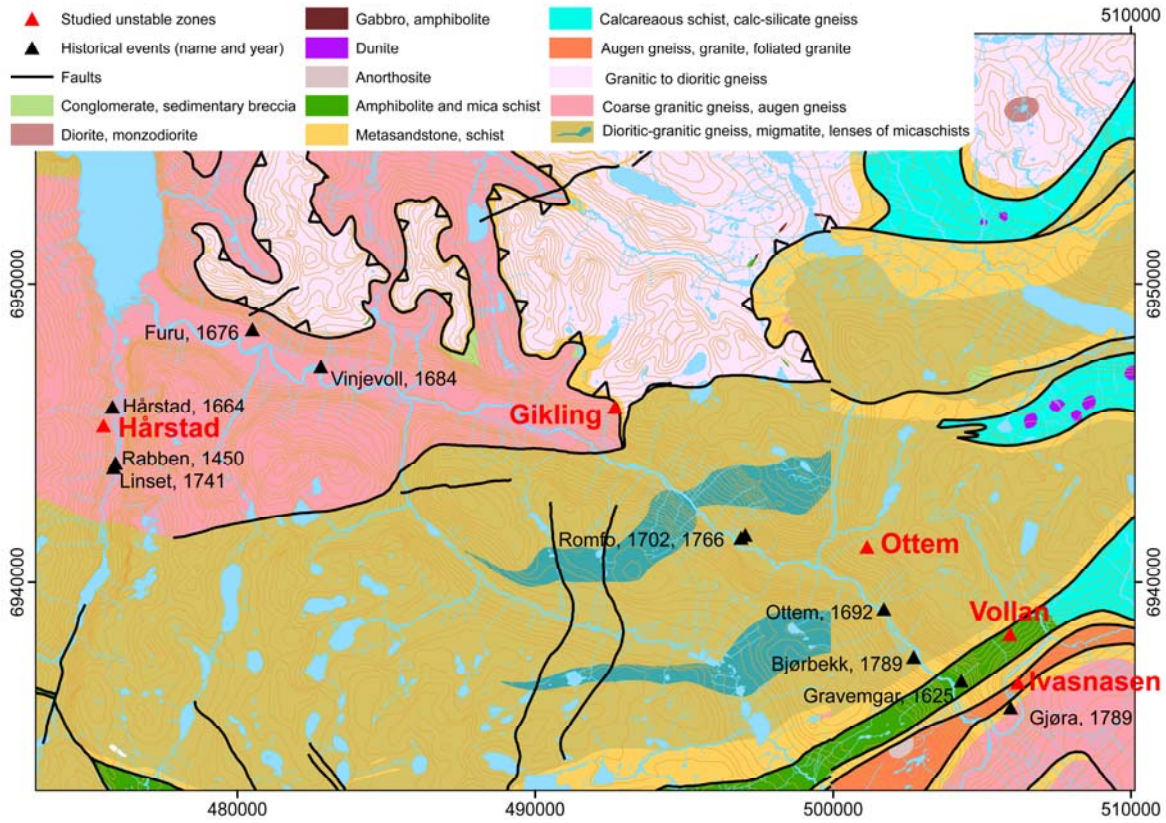

Figure 2. Studied unstable slopes and past gravitational failures in the Sunndalen valley on the geological map (scale 1 /250 000, Nilsen, O. and Wolff, 1989, Tveten et al., 1998).

2. GIKLING

Gikling is a very large unstable zone that covers an area of approximately 1 km^2 (Figure 3). The mean slope is about 25 degrees. The uppermost limit of the deformed area was mapped at a height of approximately 1400 m; we estimate the toe to lie below 900 m.

Following a short preliminary field study in 2006, Henderson and Saintot (2007) concluded that the structures at Gikling are complex and that the site would require detailed mapping in 2007. The results of the new 2007 field investigations are presented herein.
The unstable portions of the Gikling site have been divided into several (sometimes tilted and /or rotated) sub-blocks limited by large topographic depressions (Figure 3B and Figure 4). The density of opened cracks is very high; consequently, GPS points for yearly monitoring were established in 2007 (Figure 3).

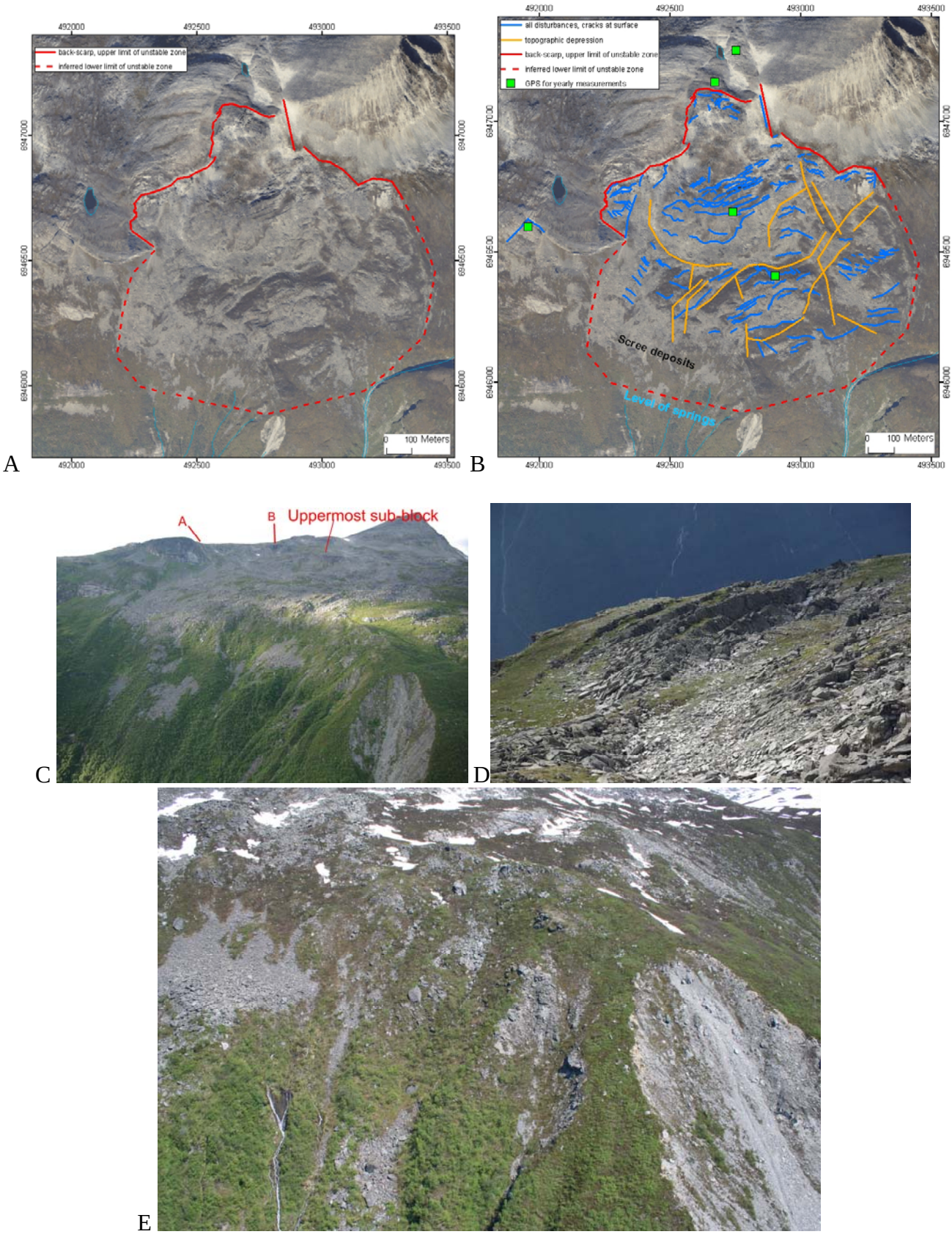

Figure 3. A and B, Orthophotos (www.norgeibilder.no) B, mapping of the structures of the large slope instability of Gikling and the GPS points set in 2007 for yearly monitoring of possible motion. C, picture from helicopter toward the north of the slope instability of Gikling. Red block letters refer to the uppermost boundaries of the slope instability as on the map of Figure 4. D, picture of the ENE-WSW cracks within the uppermost sub-block (view to the S) (the sub-block is located on picture of Figure 3C). E, Horizontal level of springs at about 800 m high (view to the NE).

The gneissic foliation is generally shallowly-dipping to the south, in places at angles approaching that of the mean topographic slope (Figure 4). Field observation suggests the uppermost limit of the slope instability to be coincident with a spatial arrangement of pre-existing structures that mark the boundary between the unstable and stable parts of the slope. (See block letters along the solid red line on Figure 4). The segments of this limit marked A, B, E and F on Figure 4 correspond to pre-existing faults (Figure 5A, B and C). Segment D (indicated on Figure 4) is the uppermost limit that we have observed. It is a wide zone of new fractures that are localized along a zone of small amplitude folds; the fracture planes are oriented parallel to the fold axes (Figure 5D). Segment C (Figure 4) is a crack several meters wide and deep, which displays stepped walls. The steps are formed by the planes of the south-dipping foliation and N-S trending steep fractures.

The lowest limit of the instability is not yet well constrained. However, a semi-horizontal line of springs is observed at about 800 m altitude (Figure 3E) and may mark the basal level of the slope instability. Therefore, the volume of the entire slope instability may be greater than 100 Mm^3. Geophysical investigations are recommended in order to determine the geometry of the structures at depth and to identify the basal plane of instability.

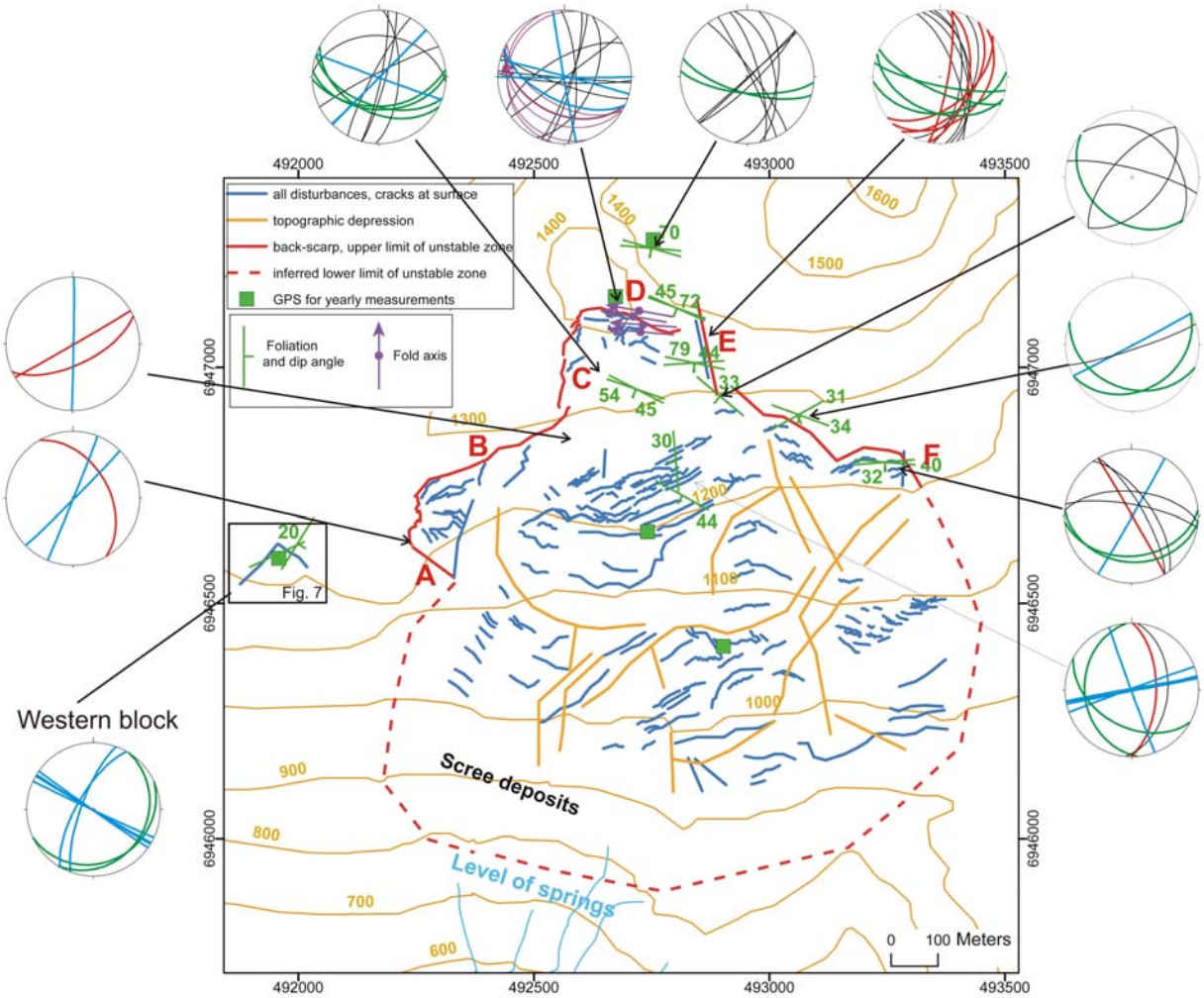

Figure 4. Detailed structural mapping of the large slope instability of Gikling and stereoplots of field measurements. Keys for stereoplots: metamorphic foliation in green, open fractures and large cracks in blue, old faults in red, fold planes and fold axes (stars) in purple, joints in black (measurements are listed in Appendix 1). In the black rectangle, location of the western block of Gikling illustrated on Figure 7.

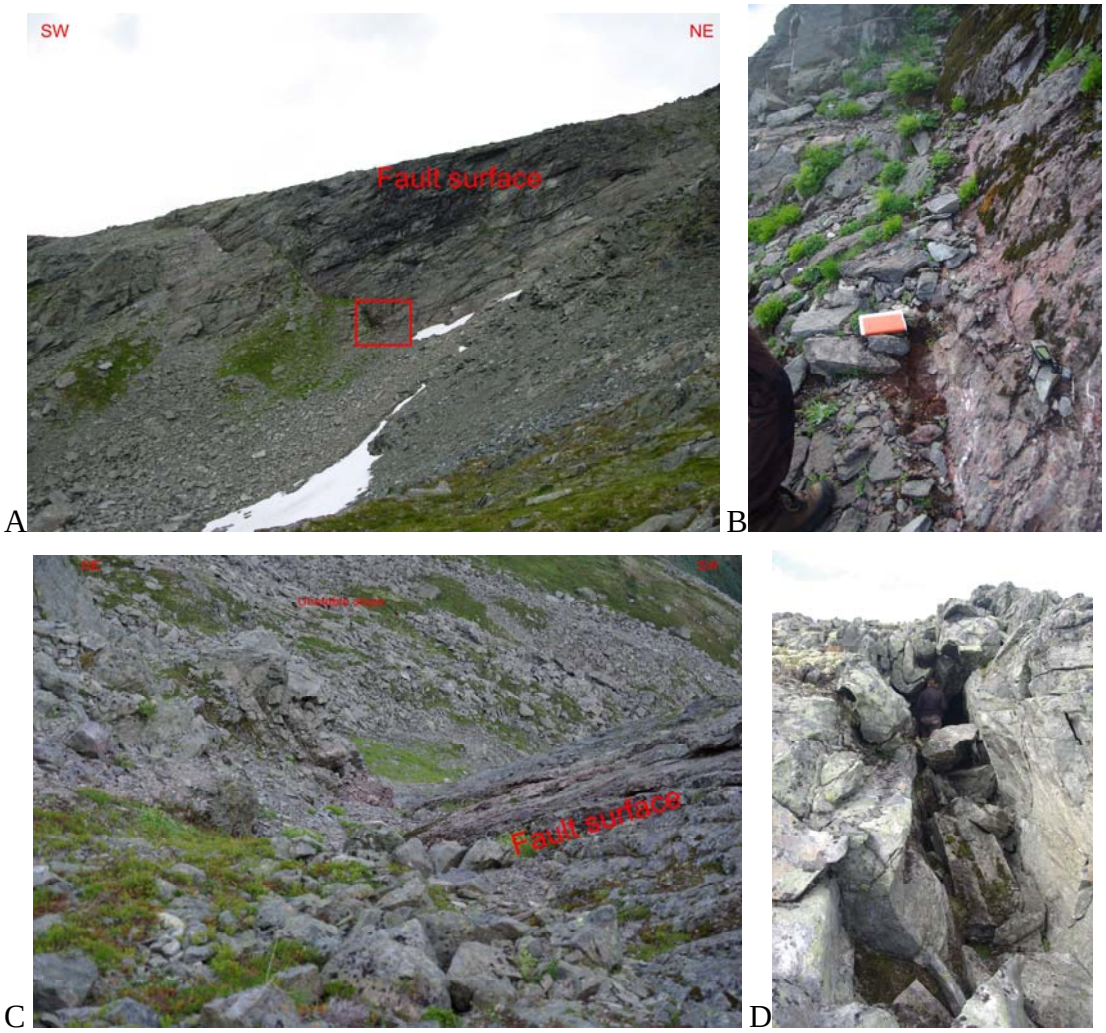

Figure 5. Pictures illustrating the reactivation of pre-existing structures that limit the slope instability. A, The limit of the unstable slope (segment B on Figure 4) as a reactivated pre-existing fault with gouge and breccia. B, Close-up of the fault with gouge and breccia (red frame on photo A) C, Reactivated pre-existing NE dipping fault (segment A as referred on Figure 4) marks a sharp border between the unstable and stable slopes. D, Localization of segment D (as referred to Figure 4) along a zone of small amplitude folds, the newly formed gravitational fractures at this place trend parallel to the azimuth of fold axes (view to west).

The genesis of the gravitational slope instability may reflect the allochthonous gneissic unit within which it developed (Figure 6). The springs at about 800 m a.s.l. may represent the trace of the basal glide plane. The springs also coincide closely with the sole detachment of the allochthon, which is composed of metasandstones and schists (Figure 6). The detachment may have developed within a weak zone that localized the base of the slope instability and acts as an aquifer.

In addition, a steep- to vertical fault zone lies at the eastern foot of the unstable zone. It separates the two autochthonous units of the valley and also limits the allochthonous sheet to the east (Figure 6). Gikling is therefore in a very peculiar structural setting that may be responsible for a weakening (perhaps by fracturing and enhanced weathering) of the gneiss unit, rendering the slope more vulnerable to gravitational forces.

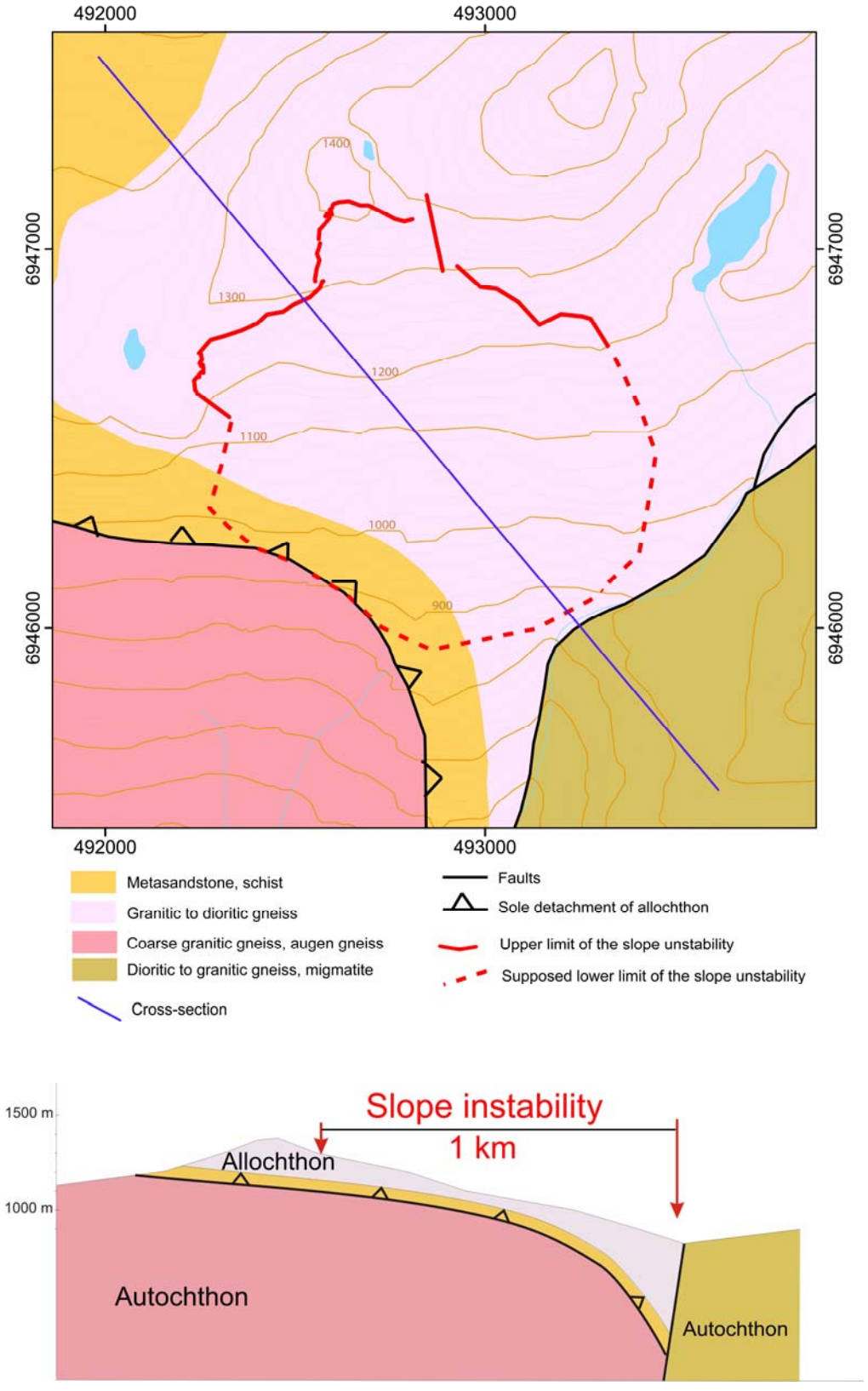

Figure 6. Geological map (Tveten et al., 1998) and cross-section showing the peculiar tectonic setting of the slope instability of Gikling.

On the western part of the area lies an unstable block on the edge of the scarp (located on Figure 4 as 'Western block'). This was identified during a reconnaissance study by Henderson & Saintot (2007). The stereoplot of structures measured at the site shows the two regional sets

of vertical fractures and (in green) the shallow dipping foliation (Figure 7). The vertical fractures are largely opened inside the unstable block and the foliation may likely be reactivated as a basal sliding plane. The total volume is estimated to be approximately 0,7 Mm^3.

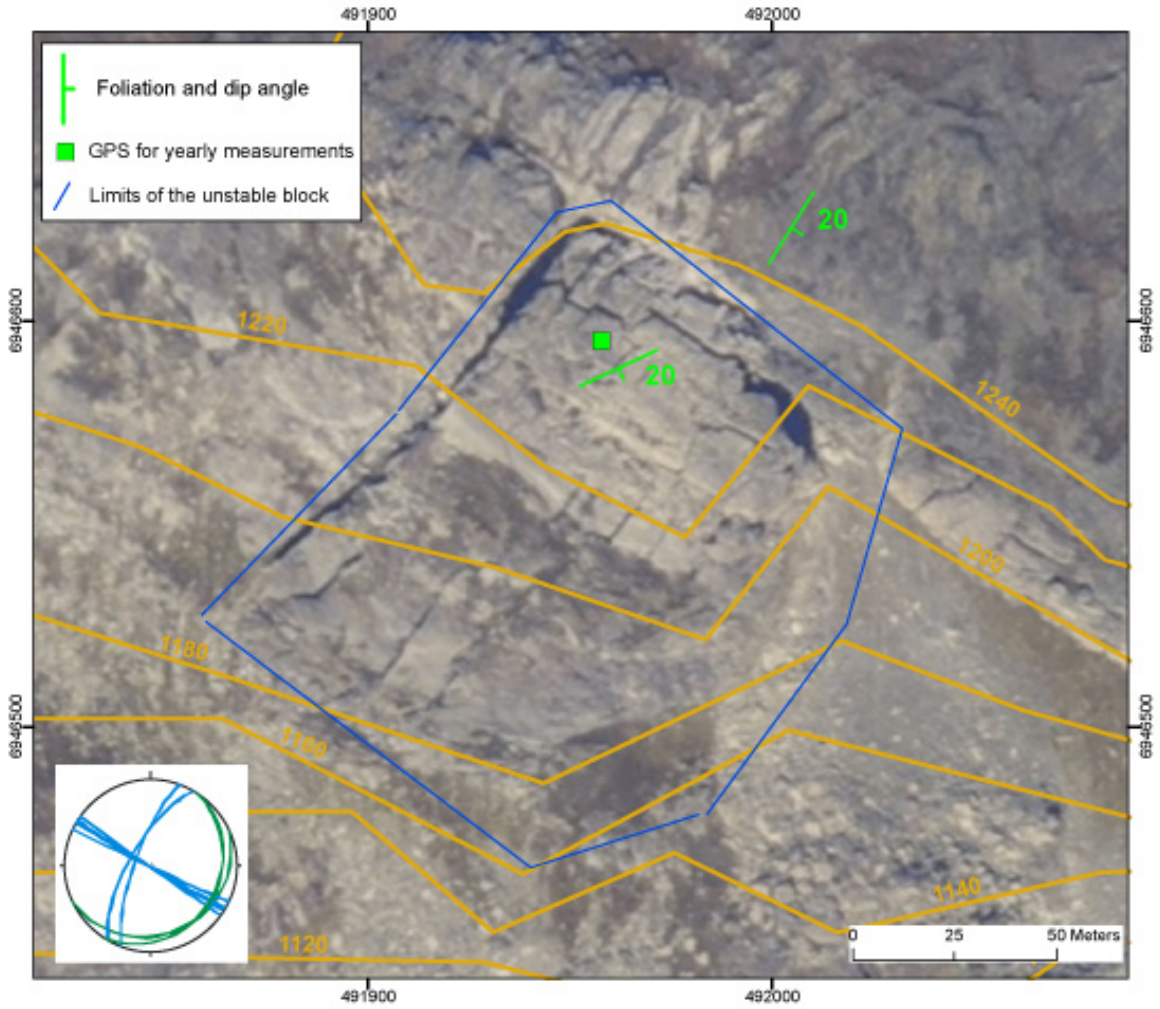

Figure 7. Orthophoto (www.norgeibilder.no) of the 'western block' of Gikling (located on map of Figure 4). Stereoplot of structures measured at this site: the destabilization of the volume occurs along the two regional sets of joints (in blue on the stereoplot), the shallow dipping foliation (in green on the stereoplot) probably acts as a basal sliding plane. The volume of the whole block is approximately 0,7 Mm^3.

3. OTTEM (Øyalykkja)

The area was first identified by E. Anda (County Geologist). Aerial photograph analyses and helicopter survey revealed further indications of recent instability (Henderson and Saintot, 2007). The maximum unstable volume was estimated to be 50 Mm^3.

The Ottem instability can be divided in three main sectors (Figure 8), each developed in autochthonous Precambrian gneisses.

The first zone is a large curved, depressed and fractured area that lies on the edge of the plateau to the east of the initially investigated area (sector 1 on Figure 8). This area has not been fully documented. The face of this zone displays recent rockfall activity, evidenced by

fresh rock surfaces along the cliff (Figure 8). If a gravitational instability has developed at the rear of the active scarp, it may have been localized along a fold hinge. This sector will require field investigations along the circular depression on the plateau in 2008.

The second unstable sector consists of scree deposits from previous failures from the edge of the plateau (sector 2 on Figure 8). These slope deposits cover a surface of approximately 125 000 m^2 on a slope dipping at 35 degrees. They contain large loose blocks that could potentially be remobilized (Figure 8, Figure 9A).

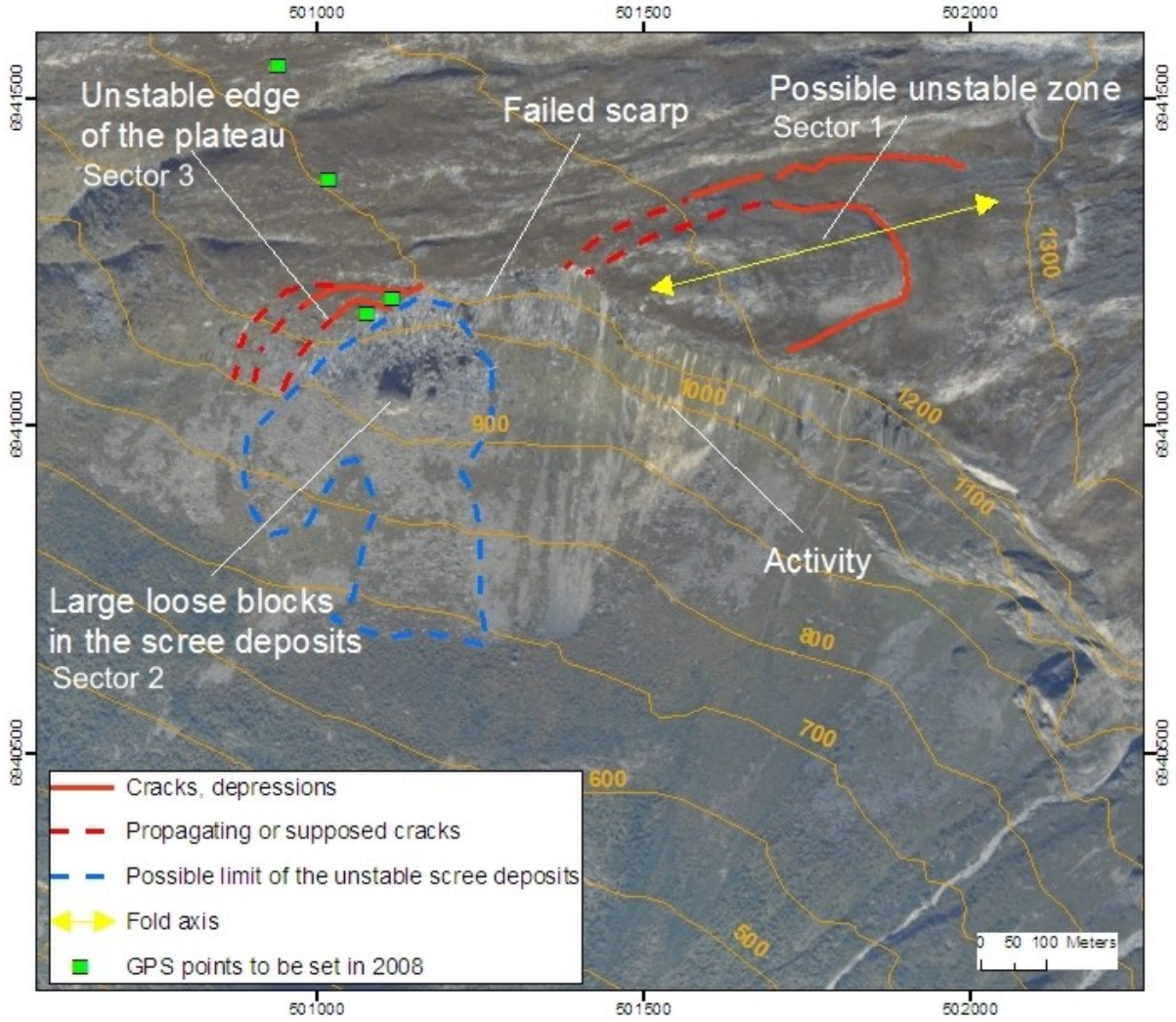

Figure 8. Orthophoto (www.norgeibilder.no) of the unstable slope of Ottem and maps of structures. On the eastern part of the studied area, a fold hinge localizes a possible large unstable zone (sector 1). Part of the scarp has already failed and the scree deposits on the slope are unstable loose material that comprises large blocks (sector 2). The western edge of the plateau at about 1000 m a.s.l. is unstable (sector 3) and cracks developed from east to west at the back.

The third unstable sector is a large block at the edge of the plateau at 1000 m a.s.l. that was investigated during the field campaign in August 2007 (sector 3 on Figure 8). The block has partially collapsed downslope by several meters. The limiting back-crack is well developed and opened on its eastern side. It forms an asymmetric graben-like structure ~5 m wide with an offset of the collapsing block ~5 meters downward (Figure 9A and B). The northern wall of the crack is stepped along a pre-existing system of roughly NNE-SSW and E-W joints

(stereoplot of Figure 10). During fieldwork we identified a zone of small amplitude folds adjacent to where the back-crack has developed (Figure 10). Elsewhere, the foliation is gently

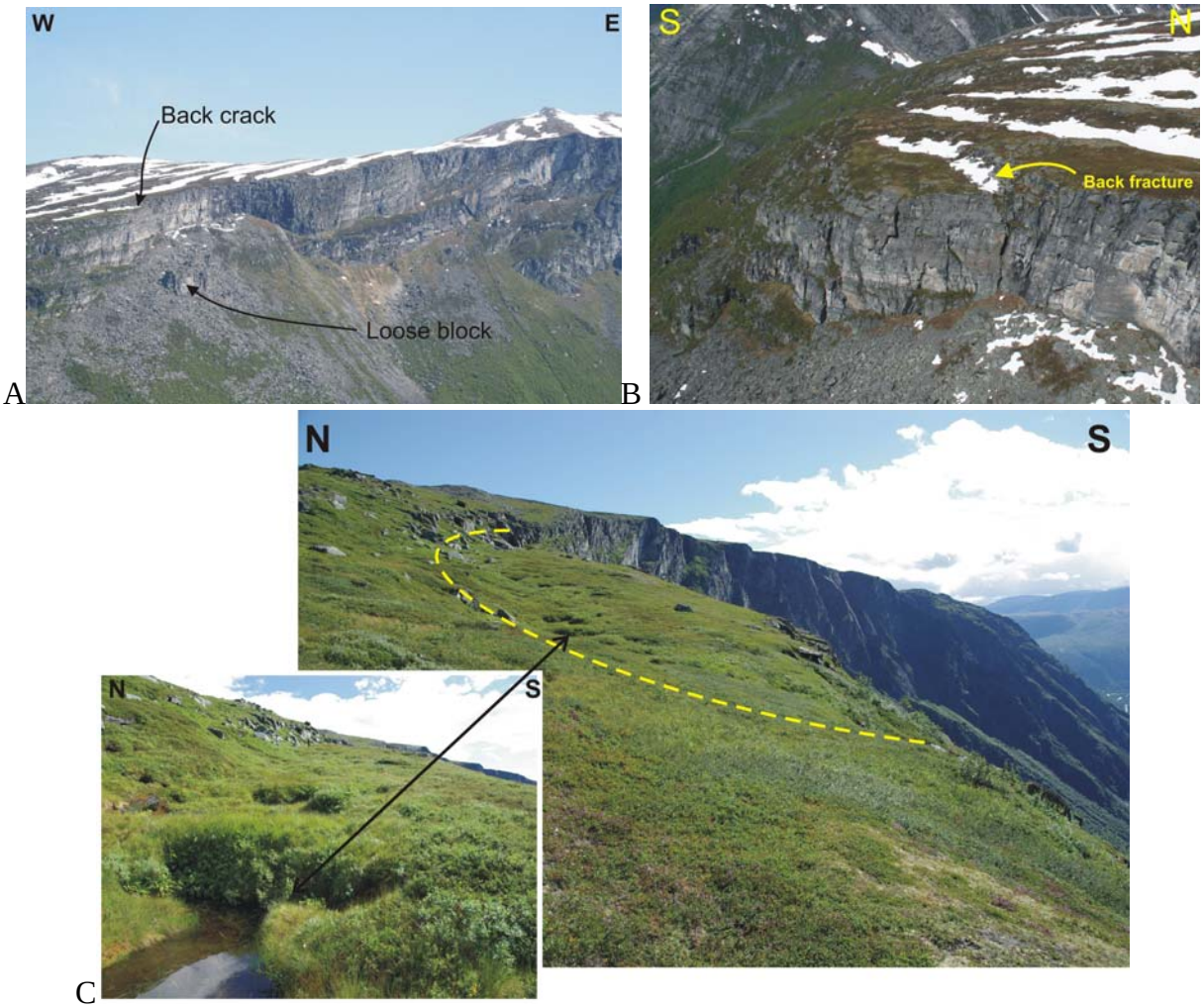

Figure 9. Field photos. A, view of the face of the unstable zone (sectors 2 and 3 of Figure 8). B, view parallel to the propagating back-fracture at the back of the unstable block (sector 3 of Figure 8). Note the large opening of the crack seen along the cliff. C, the collapsing unstable block (sector 3) with the back-crack underlined in yellow. The back-crack is well developed and opened on its eastern side whereas on the western side it is a linear depression highlighted by a series of small ponds.

dipping to the west and north-west (stereoplot of Figure 10). Failure along the edge of the plateau propagated from east to west, with evidence of previous failure(s) east of the unstable block along the same structure forming the back-crack (Figure 8). Therefore, to the west, the back-crack becomes a discrete depression highlighted by a series of small ponds (Figure 9C). The observation of the water levels in the ponds constitutes an easy monitoring method. A drop of water level of the ponds may be the result of new or expanding openings of the subjacent fractures (i.e. the back-crack), possibly related to accelerated or ongoing displacement of the unstable block. Although their levels may also fluctuate for other reasons (precipitation, snowmelt, etc), we propose that the water level of the ponds be regularly observed as a proxy for possible instability. The maximum volume of the collapsing block is estimated to be 1 Mm^3. Many open fractures parallel to the main back-crack are expressed at the surface of the large block by steps in the topography. At least one large sub-block can be shown to disintegrate into many smaller blocks in the direction of the escarpment. Also, the westernmost limit of the unstable zone may be enlarged to a discrete linear depression that we have observed on the field (Figure 10). If so, the volume of the unstable zone may be 2 Mm^3.

Four GPS positions should be established in 2008 on this unstable zone for yearly monitoring of movement (Figure 10).

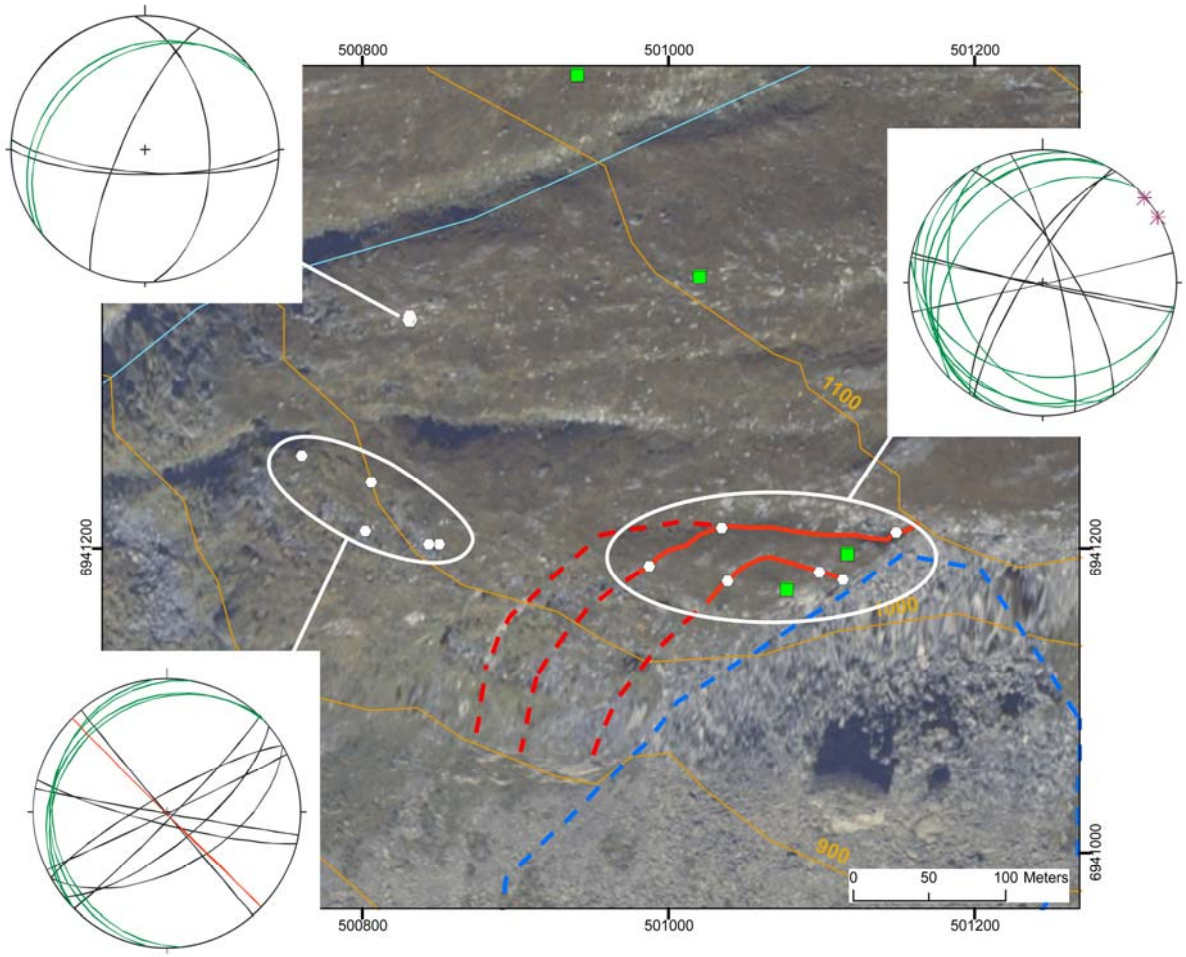

Figure 10. Stereoplots of structural data collected at Ottem on the unstable block of sector 3 (see Figure 8). Locations of field measurements as white dots; GPS points to be established in 2008 as green squares; legend for stereoplots as in Figure 4 (measurements are listed in Appendix 1). The red lines are the limits of the block. The dashed lines are the depressions seen in the field and are the supposed limits of the blocks.

4. HÅRSTAD

This locality lies on the western side of Litjdalen (Figure 1) and has been chosen for further field investigations following the helicopter survey of the Sunndalen valley and surroundings in spring 2007 (Henderson and Saintot, 2007). Results from an initial field visit conducted in summer 2007 are reported below.

The rocks at Hårstad are the coarse grained granitic gneiss of the Precambrian autochthonous basement of western Norway. NW-SE trending fractures are regionally developed (Redfield et al., 2000). The gneissic foliation is dipping ~25-30 degrees toward the valley (Tveten et al., 1998).

The potential slope instabilities appear to be of two types, localized in two different zones (Figure 11 and Figure 12A). In the first zone, two large unstable blocks, labelled A and B on Figure 11 and Figure 12A, may possibly have slid along opened shallow dipping planes parallel to foliation and toward the valley. Within block A, between the two blocks and at the back of block B, 50 to 60 degrees east-dipping open fractures may have accommodated displacement. Block A may have a total volume above 5 Mm^3; initial inspection suggests its detachment from the slope may be more advanced than that of block B (see on Figure 11). In the second zone, along the southern side of an E-W tributary river, several large columns or slices appear to have detached from the slope along NW-SE cracks (Figure 11 and Figure 12C, D and E). Their volumes are estimated to be approximately 0,25 Mm^3.

The slope instabilities of Hårstad display well-developed structures. Thus, detailed field mapping will be carried out in 2008.

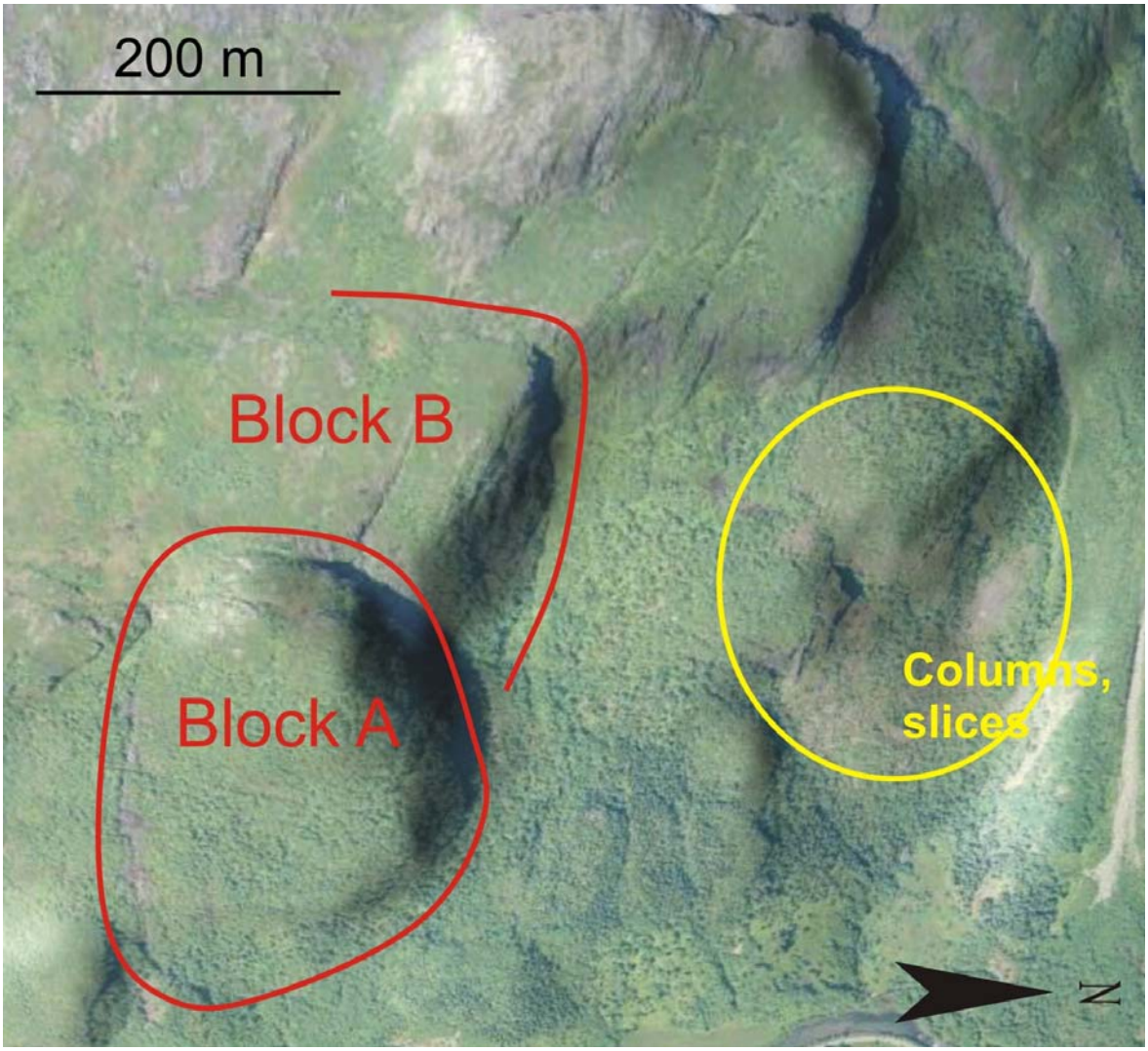

Figure 11. General top view of the site of Hårstad (from www.norgei3d.no). In the northern zone, the failure of the slope consists of columns and slices toward an E-W trending tributary river. On the southern zone, large blocks slid eastward toward the main valley on shallow east–dipping foliation, detachment of block A being more advanced than for block B.

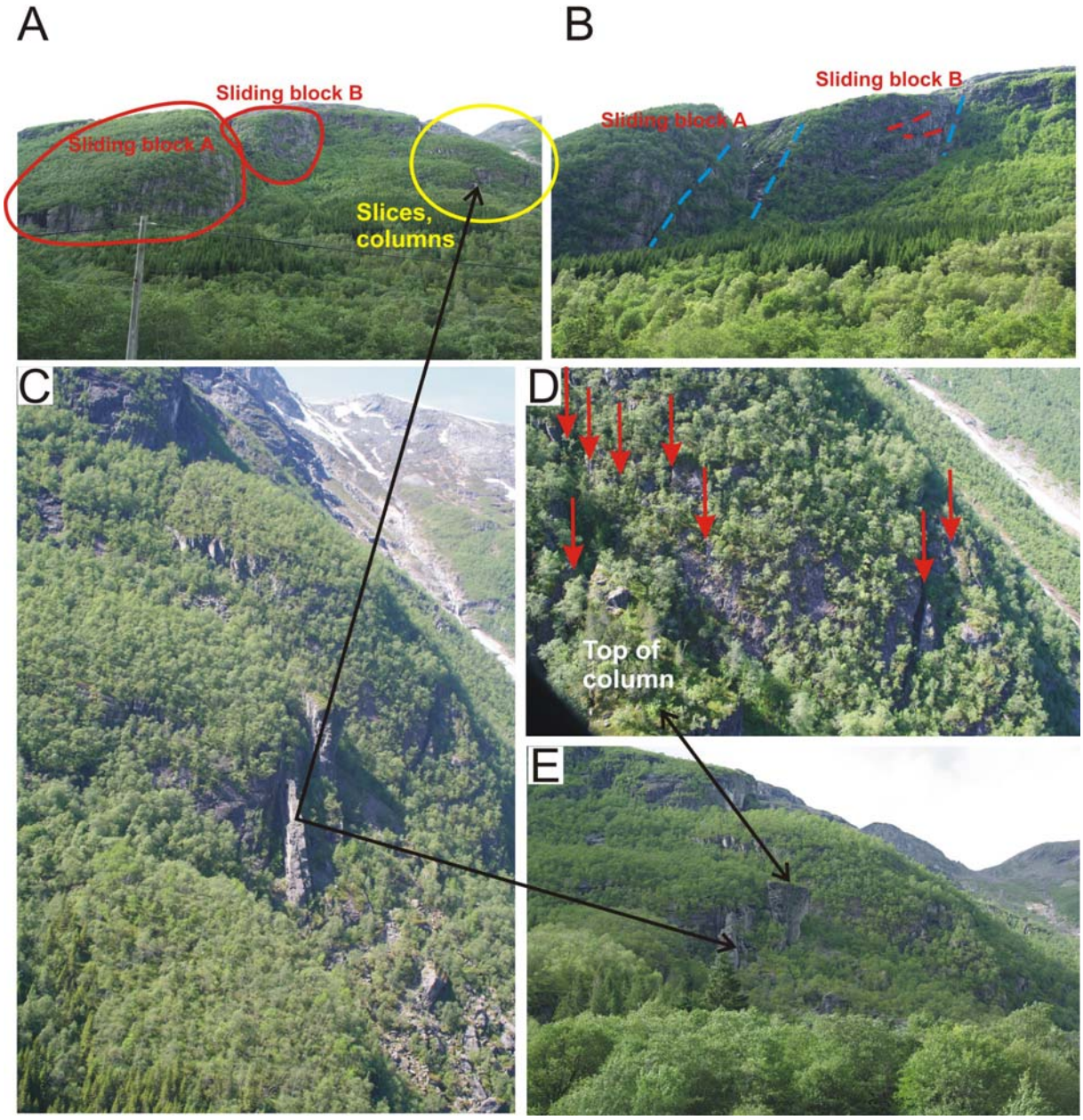

Figure 12. A, Some photos that give an overview of the site of Hårstad with the two types of instabilities (as for Figure 11, North is to the right). B, sliding blocks along reactivated shallow dipping foliation planes (in red dashed lines); open steep fractures (in blue dashed lines) testify to displacement. C, general view of the slices and columns that detached toward an E-W gully. D, NW-SE cracks (at the tip of the red arrows) along which the slices and columns detached. E, view of the large columns that detached toward the E-W gully with volumes of approximately 0,25 Mm^3.

5. IVASNASEN

During the helicopter survey of Sunndalen valley and surroundings, a slope instability was identified at Ivasnasen, close to a historical rock failure called Gjøra (Figure 1, Figure 2, Henderson and Saintot, 2007). An initial field reconnaissance at the foot of the instability was made in 2007 and is reported herein.

The geological map of the area shows that the unstable area lies in a zone of intense tectonic deformation where several thrusted units were emplaced during Caledonian times (Figure 13). Such a site will be an important natural laboratory to study the role of the pre-existing

structures in the development of slope instabilities. The slope instability itself is underlain by allochthonous augen gneiss. The site displays an old slide with a maximum failed volume of 5 Mm^3 (Figure 14A and B). The top of the failed volume was at approximately 500 m a.s.l. and the bottom of the valley is at 200 m a.s.l.. The limiting surface trends NE-SW, parallel to the thrust planes displayed on the geological map (Figure 13).

Extensive fractures appear to propagate from the previous failure limit towards the southwest and towards the northeast, possibly isolating two new unstable zones (sectors 1 and 2 on map of Figure 13 and displayed on photos of Figure 14A, B and C). The southwestern instability (sector 1) is coincident with the topographic promontory called Ivasnasen (Figure 14 A and D). The three free borders of the topographic promontory may favor the destabilization of the whole body. The estimated volume may be up to ~5 Mm^3. The limits of the slope instability to the northeast (sector 2) are not known at this time, and will be mapped in 2008.

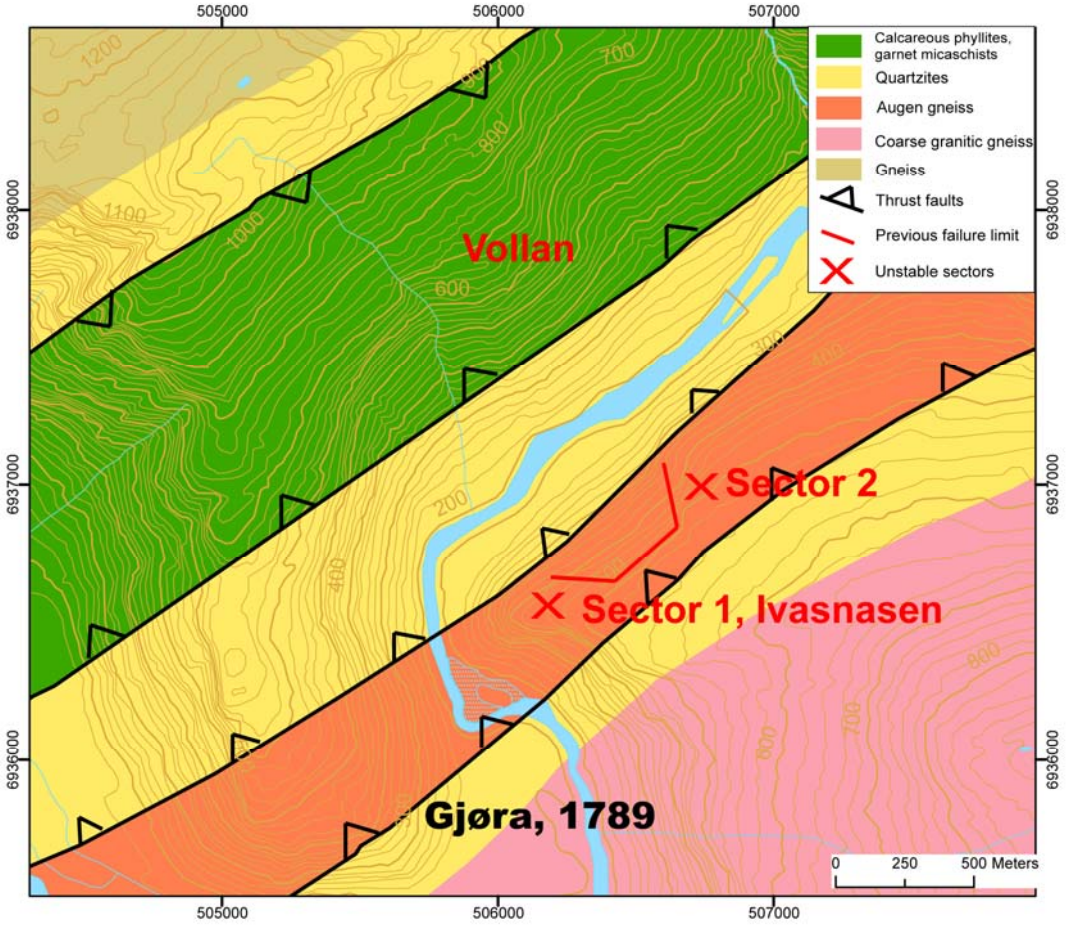

Figure 13. Geological map of Vollan and Ivasnasen surroundings (scale 1 /250 000, Nilsen, O. and Wolff, 1989). Note that sector 1 is a promontory in the topography called Ivasnasen, with three free borders that may favor the destabilization of the whole volume.

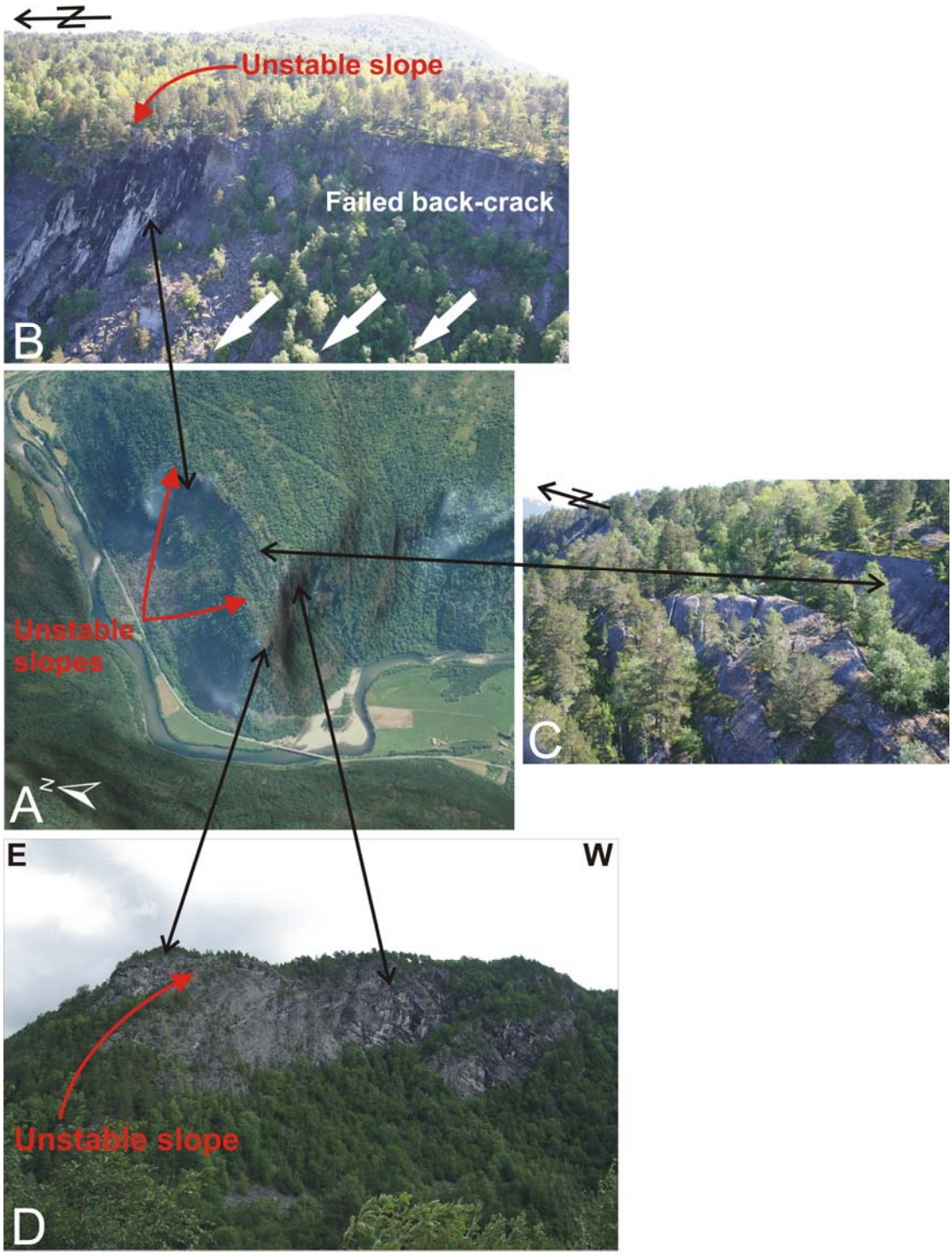

Figure 14. A, 3D view with orthophotos of the slope instability at Gjøra and Ivasnasen surroundings (www.norgei3d.no) and locations of the different parts of the instability. B, northeastern part of the limit of the previous failed volume and slope instability that propagates towards the north-east (sector 2 of Figure 13). C, southwestern slope instability called Ivasnasen (sector 1, Figure 13) and open NE-SW fractures that have propagated from the failed back-crack. D, southern face of Ivasnasen, the southwestern slope instability (sector 1 of Figure 13). The rock face displays ductile folds but also brittle structures. A detailed mapping of the site will be performed in 2008.

6. VOLLAN

This site was located during an aerial photograph survey of the Sunndalen valley. Figure 15 shows an aerial photograph with the potential minimum and maximum extent of the large potential slope instability, 1 and 2 km^2, respectively. Fieldwork will be performed at this site in 2008 for a detailed mapping of the structures and to fix the volume of the instability.

The top of the slide is located at approximately 1050 m above sea level, 850 m above the valley floor. The lower boundary of the minimum area is located 500-600 m a.s.l.. This also corresponds to a break in the shape of the slope with a shallow slope angle above this limit (<30 degrees) and a steep slope below it (Figure 16).

Based solely on the width of the back scarp, the horizontal displacement may be in the order of 100 m. Given the arcuate shape of the cracks that have developed within the instability, it appears that most of the displacement was accommodated by creep as a 'semi-ductile downward flow' (Figure 15). Towards the valley floor, a cover of scree deposits is observed, which may indicate that parts of the slope have already failed. The deposits are probably responsible for the deviation of the stream of the river south of the instability (Figure 15). These deposits may also cover the toe of the largest unstable area (Figure 15).

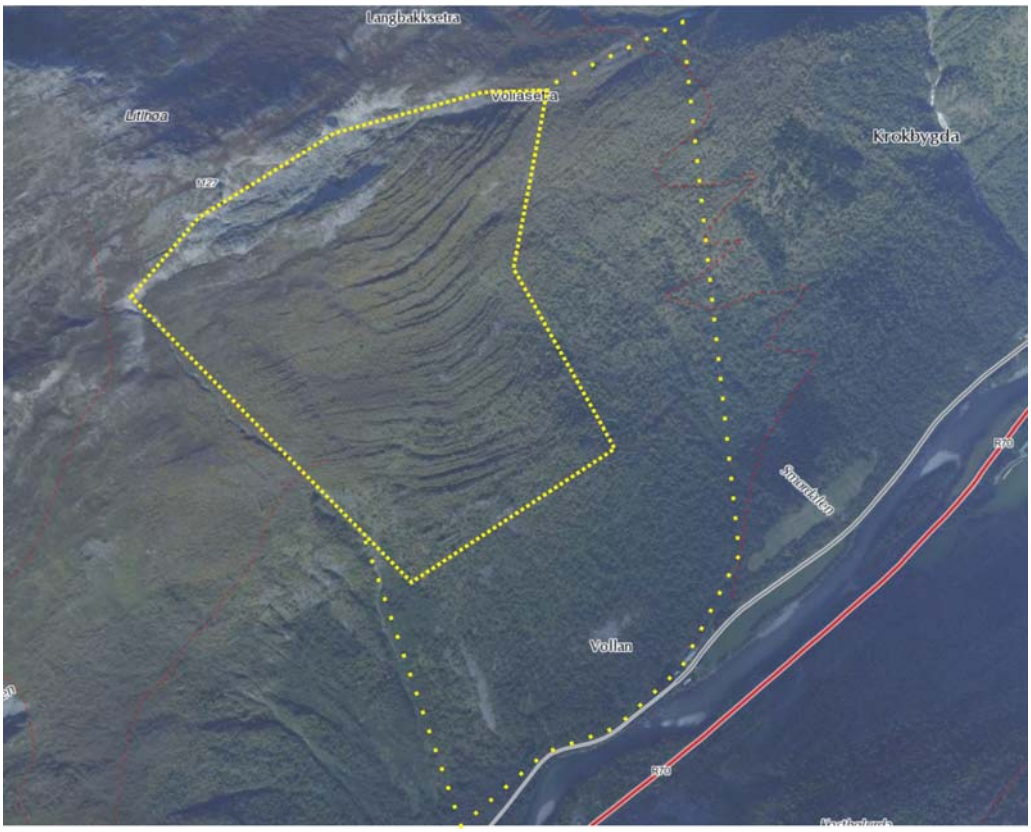

Figure 15. Aerial photograph of the Vollan site with indications of minimum and maximum boundaries of the slope instability. (www.norgeibilder.no)

The bedrock map (see Figure 13) indicates that the slope instability is located in a allochthonous sheet of micaschists and that its back-scarp may coincide with a NE-SW trending thrust plane. The foliation in the area is sub-vertical and parallel to the valley.

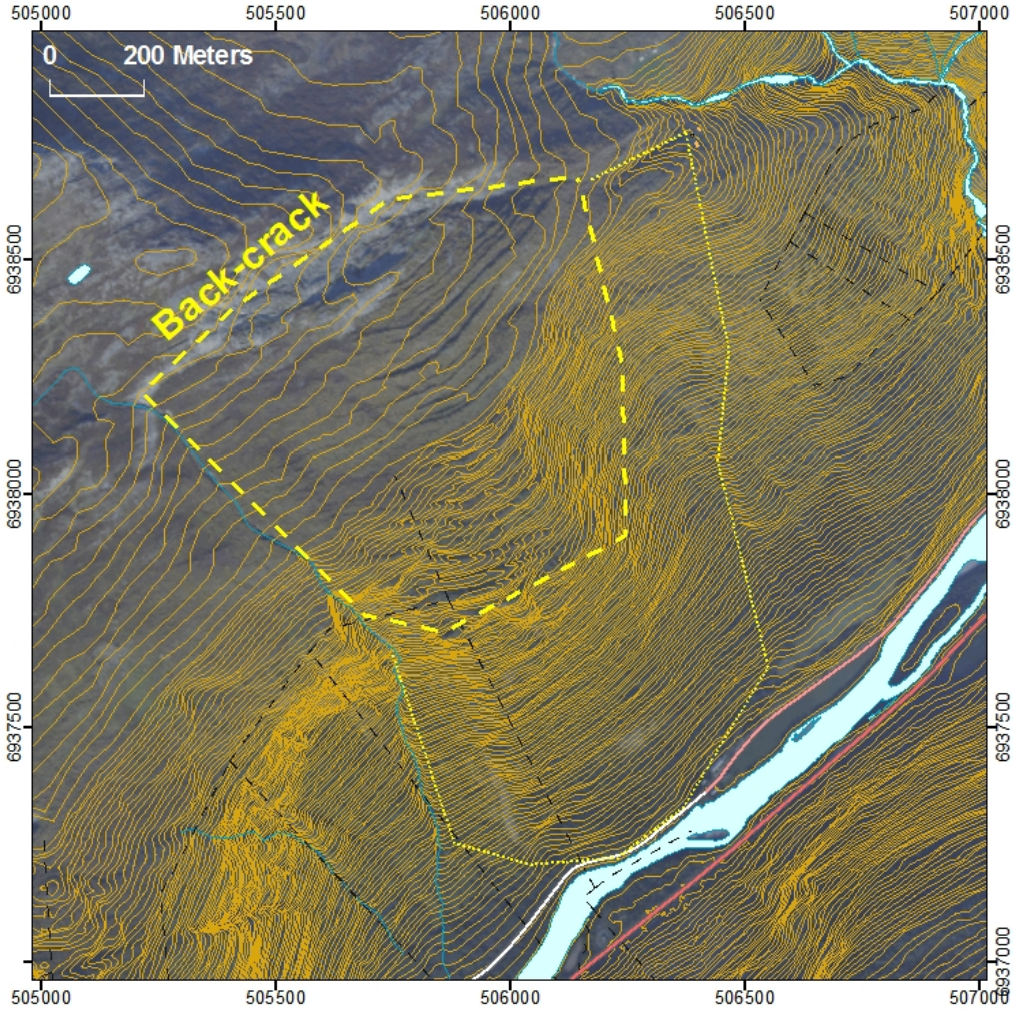

Figure 16. Topographic map of the Vollan site showing the break of the slope angle.

CONCLUSION

Four sites have been investigated along the Sunndalen valley following a helicopter survey of the valley and surroundings in 2007. A fifth site was detected subsequently by aerial photograph analysis.

1. Gikling is a large slope instability of more than 100 Mm^3. Surface mapping has highlighted the role of the pre-existing geological setting in the development of slope tectonics. Further sub-surface geophysical investigations could better define the depth of the unstable volume, and should be conducted. GPS positions have been set in 2007 to enable yearly monitoring of possible movements. These will be measured again in 2008 to determine if there is movement.

2. Ottem can be subdivided into three zones. The first and larger zone should be studied in 2008. It lies at the edge of the high plateau. Destabilization may correspond with the presence of a large fold hinge containing large fractures that can be observed from aerial photographs. The second unstable zone comprises scree deposits covering a surface area of 125 000 m^2 on a slope dipping approximately 35 degrees. The third unstable zone is due to propagation of

the gravitational deformation from a previous failed scarp, itself probably the source of the scree deposits. This unstable zone is sub-divided in three main blocks with a total volume of 2 Mm^3. The degree of disintegration of rock bodies within the zone increases towards the cliff where many unstable smaller columns and slices can be seen along the face. Four positions have been chosen to set GPS points in 2008 for a future yearly monitoring of the whole unstable volume.

3. Hårstad contains two types of slope instabilities: rockslides with basal shear planes parallel to foliation with a volume of 5 Mm^3 for the largest block and columnar failures along NW-SE large cracks with a volume of 0,25 Mm^3 for the largest columns. Further field investigations are planned in 2008 on the site to observe the degree of slope activity.

4. Close to an historical slope failure at Gjøra, two slope instabilities are observed along the NE-SW trending river and on the south-eastern slope of the valley. Both appear to result from a steep extensive fracture system stemming from a previous failed volume of some 5 Mm^3. The limit of the northern unstable zone is not defined. The southern instability called Ivasnasen is a topographic promontory, with three free borders. Ivasnasen appears to be currently detaching from the slope by a set of back-bounding fractures. The volume may be up to 5 Mm^3. Further field studies are planned in 2008 to map the extent of the site.

5. Another instability, called Vollan, on the western side of the same NE-SW trending river, has been identified on aerial photographs. Vollan displays a large deformed surface of 1 to 2 km^2 that will be investigated in the field in 2008.

The development of the two slope instabilities (Vollan and Ivasnasen) along the NE-SW trending river is probably due to its tectonic setting, with a narrow NE-SW band of squeezed allochthonous units that appear to control the relief and the drainage patterns. In this model, the NE-SW pre-existing tectonic structures localized the development of the NE-SW gravitational fractures.

Acknowledgements

Thanks to Iain Henderson and Marc-Henri Derron for reviewing the report and fruitful discussion on the topic.

References

Henderson, I.H.C., and Saintot, A., 2007. Fjellskredundersøkelser i Møre og Romsdal. NGU report 2007.043, 68 pp.

Nilsen, O. and Wolff, F.C. 1989. Geologisk kart over Norge, berggrunnskart Røros og Sveg, 1: 250 000, NGU.

Redfield, T. F., Gabrielsen, R. H., & Torsvik, T. 2000. Fracture lineaments, Cenozoic(?) faults, and Mesozoic extensional tectonics of the Møre Trøndelag region, central Norway, *NGU Open File Report*, 2000.070, 21p.

Tveten, E., Lutro, O., Thorsnes, T. 1998. Geologisk kart over Norge, berggrunnskart Ålesund, 1: 250 000, NGU.

APPENDIX 1. Table of structural field data.

Site	Easting	Northing	Strike	Dip angle	Azimuth	Plunge	Structure
Gikling	492234	6946631	330	45			Fault/ lineament, reddish plane
Gikling	492261	6946673	45	88			Crack
Gikling	492261	6946673	22	89			Crack
Gikling	492521	6946861	65	64			Fault, with red gouge and breccia
Gikling	492600	6947017	110	89			Open joint
Gikling	492625	6946768	60	89			Fault
Gikling	492625	6946768	1	89			Crack
Gikling	492633	6946998	45	89			Stepped cracks opened along NS joints and south-dipping foliation
Gikling	492692	6946967	45	89			Crack
Gikling	492702	6947117			275	10	Fold axis
Gikling	492702	6947117			280	12	Fold axis
Gikling	492702	6947117			274	22	Fold axis
Gikling	492702	6947117			280	20	Fold axis
Gikling	492702	6947117			278	10	Fold axis
Gikling	492702	6947117	90	89			Back-crack, scarp
Gikling	492702	6947117	170	89			Scarp
Gikling	492702	6947117	53	89			Joint
Gikling	492702	6947117	120	55			Fold axial plane
Gikling	492702	6947117	93	83			Joint
Gikling	492702	6947117	115	60			Uppermost large crack
Gikling	492702	6947117	190	15			Axial plane
Gikling	492702	6947117	120	30			Axial plane
Gikling	492702	6947117	109	80			Joint
Gikling	492702	6947117	15	80			Joint
Gikling	492702	6947117	240	67			Joint
Gikling	492702	6947117	20	82			Joint
Gikling	492702	6947117	25	54			Joint
Gikling	492702	6947117	95	89			Joint
Gikling	492702	6947117	160	15			Axial plane
Gikling	492702	6947117	285	89			1,5 m wide crack
Gikling	492702	6947117	115	43			Axial plane
Gikling	492702	6947117	357	76			Joint
Gikling	492710	6946710	40	89			Fracture
Gikling	492713	6946945	117	45			Metamorphic foliation
Gikling	492713	6946945	3	66			Joint
Gikling	492713	6946945	15	82			Joint
Gikling	492713	6946945	274	38			Joint

Gikling	492713	6946945	208	82			Joint
Gikling	492713	6946945	109	54			Metamorphic foliation
Gikling	492713	6946945	243	85			Joint
Gikling	492747	6947244	106	70			Metamorphic foliation
Gikling	492747	6947244	46	88			Joint
Gikling	492747	6947244	48	89			Joint
Gikling	492747	6947244	349	56			Joint
Gikling	492747	6947244	95	70			Metamorphic foliation
Gikling	492747	6947244	10	52			Joint
Gikling	492747	6947244	345	75			Joint
Gikling	492747	6947244	334	86			Joint
Gikling	492747	6947244	324	82			Joint
Gikling	492747	6947244	46	80			Joint
Gikling	492792	6946800	175	30			Metamorphic foliation
Gikling	492792	6946800	1	60			Chlorite fault
Gikling	492792	6946800	80	89			Crack
Gikling	492792	6946800	5	45			Joint
Gikling	492800	6947117	110	45			Metamorphic foliation
Gikling	492800	6947117	114	72			Metamorphic foliation
Gikling	492809	6947229	10	80			Old epidote rich fault
Gikling	492809	6947229	35	46			Old epidote rich fault
Gikling	492809	6947229	45	32			Old epidote rich fault
Gikling	492809	6947229	52	52			Old epidote rich fault
Gikling	492809	6947229	10	54			Old epidote rich fault
Gikling	492809	6947229	6	64			Joint
Gikling	492809	6947229	355	55			Joint
Gikling	492809	6947229	351	52			Joint
Gikling	492809	6947229	345	58			Joint
Gikling	492809	6947229	340	70			Joint
Gikling	492809	6947229	23	48			Joint
Gikling	492810	6946720	119	44			Metamorphic foliation
Gikling	492810	6946720	80	89			Fracture
Gikling	492840	6947000	86	44			Metamorphic foliation
Gikling	492840	6947000	102	79			Metamorphic foliation
Gikling	492851	6946791	250	89			Large crack
Gikling	492851	6946791	260	89			Large crack
Gikling	492889	6946931	130	33			Metamorphic foliation, wall of graben-like structure
Gikling	492889	6946931	41	52			Joint, steps
Gikling	492889	6946931	284	79			Joint
Gikling	492889	6946931	313	33			Joint
Gikling	492889	6946931	221	64			Joint
Gikling	492900	6946770	160	89			Extension cracks

Gikling	493062	6946889	62	89			Extension crack
Gikling	493062	6946889	72	84			Joint
Gikling	493062	6946889	110	34			Metamorphic foliation
Gikling	493062	6946889	61	31			Metamorphic foliation
Gikling	493148	6946474	290	89			Large crack not so deep not so active
Gikling	493245	6946789	85	40			Metamorphic foliation
Gikling	493245	6946789	330	75			Joint
Gikling	493245	6946789	275	60			Joint
Gikling	493245	6946789	280	76			Joint
Gikling	493245	6946789	325	65			Joint
Gikling	493245	6946789	95	32			Metamorphic foliation
Gikling	493278	6946782	30	89			Fracture
Gikling	493278	6946782	330	89			Old epidote rich fault
Gikling 'western block'	491958	6946595	65	20			Metamorphic foliation
Gikling 'western block'	491958	6946595	120	89			Open joint
Gikling 'western block'	491958	6946595	200	75			Open joint
Gikling 'western block'	491958	6946595	210	70			Open joint
Gikling 'western block'	491958	6946595	115	89			Open joint
Gikling 'western block'	491958	6946595	120	89			Open joint
Gikling 'western block'	492006	6946622	125	89			Opened fractures
Gikling 'western block'	492006	6946622	32	20			Foliation
Ottem	500806	6941244	225	20			Metamorphic foliation
Ottem	500806	6941244	228	17			Metamorphic foliation
Ottem	500806	6941244	240	80			Joint
Ottem	500806	6941244	50	70			Joint
Ottem	500806	6941244	135	89			Fault
Ottem	500830	6941350	235	25			Metamorphic foliation
Ottem	500830	6941350	235	25			Metamorphic foliation
Ottem	500830	6941350	230	30			Metamorphic foliation
Ottem	500830	6941350	356	50			Joint
Ottem	500830	6941350	204	76			Joint
Ottem	500830	6941350	94	76			Joint
Ottem	500830	6941350	90	75			Scarp
Ottem	500844	6941203	174	15			Metamorphic foliation
Ottem	500844	6941203	100	89			Joint
Ottem	500844	6941203	104	82			Joint
Ottem	500844	6941203	44	86			Joint
Ottem	500844	6941203	60	55			Joint
Ottem	500850	6941203	190	13			Metamorphic foliation
Ottem	500850	6941203	64	90			Joint
Ottem	500850	6941203	100	90			Joint
Ottem	500850	6941203	140	90			Joint
Ottem	501039	6941179	211	80			Joint

Ottem	501099	6941185			60	1	Fold axis
Ottem	501149	6941211	119	11			Metamorphic foliation
Ottem	501149	6941211	209	20			Metamorphic foliation
Ottem	501149	6941211	193	14			Metamorphic foliation
Ottem	501149	6941211	153	35			Metamorphic foliation
Ottem	501149	6941211	100	30			Metamorphic foliation
Ottem	501149	6941211	224	36			Metamorphic foliation
Ottem	501149	6941211	147	14			Metamorphic foliation
Ottem	501149	6941211	206	20			Metamorphic foliation
Ottem	501149	6941211	101	89			Joint
Ottem	501149	6941211	328	72			Joint
Ottem	501149	6941211	103	88			Joint
Ottem	501149	6941211	77	89			Joint
Ottem	501149	6941211	346	80			Joint
Ottem	501149	6941211	213	72			Joint
Ottem	501149	6941211			50	1	Fold axis